Table 10 Analytical results from ammonium acetate leach

Sample Number	KR-1	DT-1	DEL-WS12-S	DEL-WS3-S	H-S7	Matrix Blank	Detection Limit
Lab No.	1126	1127	1128	1129	1130		
As	2.6	0.3	0.6	0.7	0.9	<0.2	0.2
Sn	<2.0	<2.0	<2.0	<2.0	<2.0	<2.0	2.0
Mo	8	0.5	9.2	0.7	11.0	<0.5	0.5
Cr	<10	<10	<10	<10	<10	<10	10
Zn	2900	47	240	93	220	<0.1	0.1
Cd	1.2	<0.5	1.9	0.8	37	<0.5	0.5
Pb	8	4	35	27	19.0	<1	1
Ba	2000	350	1600	510	1000	<1	1
Co	2300	3.8	110	35	2.1	<0.2	0.2
Fe	<30	<30	<30	<30	<30	<30	30
SiO2	5600	8200	800	800	10000	<50	50
B	<50	<50	<50	<50	<50	<100	100
Mn	900	<10	4000	1100	<10	<10	10
V	<20	<20	<20	<20	<20	<20	20
Cu	2900	14	590	940	140	<20	0.2
La	24	1.6	2.2	3.5	210	<0.1	0.1
Ni	530	<5	<5	<5	<5	<0.1	0.1
Y	5.5	0.2	1.1	1.6	1.1	<5	5
Al	110	<10	30	<10	10	<0.1	0.1
Sr	300	61	130	81	36	<10	10
Ag	<0.1	0.1	3	<0.1	0.2	<0.1	0.1
SO4, mg/L	72	570	55	140	140	<1	1

Results expressed as ug/L unless otherwise specified.

6 Modelling

6.1 Hydrogeology

Parameters for groundwater flow modelling

Hydraulic conductivity values were calculated from water level recovery tests performed on many of the piezometers after sampling. Data from Banks R, N and H were analysed using the Hvorslev recovery test method for an unconfined, partially-penetrating well (Hvorslev 1951). The hydraulic conductivity of the sediments around each well was assumed to be isotropic for the purpose of the Hvorslev analysis (table 12). In Bank D and the north and south lobes of the delta, where recovery rates of water levels were too rapid to measure by hand, a minimum hydraulic conductivity value was estimated based on the amount of groundwater removed and a recovery time of about 20 s. Results and equations used are included in table 12. Data used to determine the value T_0 (see table 12) for each Hvorslev analysis are included in table 13 and figure 25.

Hydraulic conductivity values of sediments in the higher banks, Banks H, N and R, were significantly lower ($K = 7x10^{-8}$ to $1x10^{-6}$ m/s; table 12) than those estimated for sediments further downstream, Bank D and the north and south lobes of the delta ($K \approx 1x10^{-4}$ m/s, table 12). Some of the variation in hydraulic conductivity values measured in the higher banks is probably due to smearing of clay particles in the monitoring interval during drilling. This would reduce the apparent hydraulic conductivity of the sediments immediately surrounding the

Table 11 pH, conductivity and redox potential results from ammonium acetate leach

Conductivity

Sample Number	KR-1	DT-1	DEL-WS12-S	DEL-WS3-S	H-S7	Matrix Blank
Lab No.	1126	1127	1128	1129	1130	
5 min	41000	42000	40000	46000	67000	42000
30 min	47000	45000	45000	48000	43000	46000
1 hr	49000	60000	49000	47000	86000	51000
1.5 hrs	52000	53000	55000	53000	92000	52000
2 hrs	52000	54000	54000	54000	90000	53000
2.5 hrs	53000	50000	52000	52000	85000	51000
4 hrs	51000	48000	46000	50000	91000	50000
6 hrs	51000	50000	50000	51000	90000	51000
22 hrs	53000	55000	54000	54000	90000	53000
24 hrs	54000	52000	55000	55000	90000	55000

Results are expressed as uS/cm unless otherwise specified.

pH

Sample Number	KR-1	DT-1	DEL-WS12-S	DEL-WS3-S	H-S7	Matrix Blank
Lab No.	1126	1127	1128	1129	1130	
5 min	6.7	6.5	6.9	6.8	7.0	6.9
30 min	6.7	6.6	6.8	6.7	7.0	6.9
1 hr	6.7	6.6	6.9	6.8	7.0	6.9
1.5 hrs	6.7	6.6	6.9	6.8	7.0	6.9
2 hrs	6.7	6.5	6.8	6.7	7.0	6.9
2.5 hrs	6.7	6.5	6.9	6.8	7.0	6.9
4 hrs	6.7	6.5	6.8	6.7	7.0	6.9
6 hrs	6.7	6.5	6.9	6.7	6.9	6.9
22 hrs	6.7	6.5	6.9	6.7	6.9	6.9
24 hrs	6.7	6.5	6.9	6.7	7.0	6.9

Results are expressed as units unless otherwise specified.

Eh - Redox Potential

Sample Number	KR-1	DT-1	DEL-WS12-S	DEL-WS3-S	H-S7	Matrix Blank
Lab No.	1126	1127	1128	1129	1130	
5 min	218	182	204	209	194	224
30 min	210	193	217	212	202	233
1 hr	206	206	216	222	207	239
1.5 hrs	209	220	228	234	213	241
2 hrs	202	222	226	233	219	241
2.5 hrs	214	227	234	233	211	241
4 hrs	211	229	214	232	225	241
6 hrs	207	234	219	225	210	239
22 hrs	206	227	207	234	225	240
24 hrs	211	234	213	238	224	241

Results are expressed as millivolts(mV) unless otherwise specified.

Table 12 Hydraulic conductivity values

Volume of fluid removed from piezometers

Location	Sampled volume (ml)	Total volume removed (ml)	Well ID	Water volume/ linear metres			Decline in head (cm)
				(m3/m)	ml/m	x cm/100ml	
N,H, R	1000+150	1150	25 mm	0.000490874	491	20.37	234.28
	1000+200	1200	25 mm	0.000490874	491	20.37	244.46
Delta	1000	1000	40 mm	0.001256637	1257	7.96	79.58
R-W2S	750+150+150	1050	25 mm	0.000490874	491	20.37	213.90
R-W1S	500+150+150	800	25 mm	0.000490874	491	20.37	162.97
R-W3	500+250+200+150	1100	25 mm	0.000490874	491	20.37	224.09
N-W1	750+100+150	1000	25 mm	0.000490874	491	20.37	203.72
N-W2	750+40+150	940	25 mm	0.000490874	491	20.37	191.50
H-W1	750+225+150	1125	25 mm	0.000490874	491	20.37	229.18
D-W1	750+225	975	40 mm	0.001256637	1257	7.96	77.59
D-W2	750+225	975	40 mm	0.001256637	1257	7.96	77.59
D-W3	750+225	975	40 mm	0.001256637	1257	7.96	77.59

Unconfined partially-penetrating well:

For mL/R>8: K=(r^2ln(mL/2R))/(2LTo)
(Hvorslev, 1951)

where:

r (cm)	piezometer casing radius
L (cm)	length of open zone
R (cm)	radius of open zone
K (cm/s)	hydraulic conductivity
To (s)	time where (H-h)/(H-Ho)=0.37 (semi-log)
m	SQRT(Kh/Kv) assumed = 1 (isotropic hydraulic conductivity)

Piezometer	R (cm)	L (cm)	L/R	r (cm)	To (s)	Calculated K (cm/s)	Calculated K (m/s)	Calculated K (m/d)
Bank R								
R-WS1	1.25	37.3	29.84	1.25	5800	9.76E-06	9.76E-08	0.008
R-WD1	1.25	30	24.00	1.25	2000	3.24E-05	3.24E-07	0.028
R-WS2	1.25	29.4	23.52	1.25	1200	5.46E-05	5.46E-07	0.047
R-WD2	1.25	29	23.20	1.25	1000	6.60E-05	6.60E-07	0.057
R-W3	1.25	30	24.00	1.25	800	8.09E-05	8.09E-07	0.070
Bank N								
N-W1	1.25	36	28.80	1.25				
N-W2	1.25	32	25.60	1.25				
N-W3	1.25	36	28.80	1.25	800	7.24E-05	7.24E-07	0.063
N-W4	1.25	35	28.00	1.25	600	9.82E-05	9.82E-07	0.085
Bank H								
H-W1	1.25	30.5	24.40	1.25	9600	6.67E-06	6.67E-08	0.006
H-WS2	1.25	29	23.20	1.25	9200	7.18E-06	7.18E-08	0.006
H-WD2	1.25	29	23.20	1.25	4600	1.44E-05	1.44E-07	0.012
H-W3	1.25	31	24.80	1.25	2900	2.19E-05	2.19E-07	0.019
Bank D								
D-W1	2.00	32	16.00	2.00				
D-W2	2.00	35	17.50	2.00		NO DATA		
D-W3	2.00	31	15.50	2.00				
N Delta								
DEL-WS1	2.00	36	18.00	2.00				
DEL-WD1	2.00	36.8	18.40	2.00				
DEL-WS2	2.00	38	19.00	2.00				
DEL-WS3	2.00	36.1	18.05	2.00		Recovery times assumed for all delta wells:		
DEL-WS4	2.00	37	18.50	2.00				
DEL-WS5	2.00	37	18.50	2.00	10 seconds recovery time			
DEL-WS6	2.00	36.5	18.25	2.00	1.4	8.72E-02	8.72E-04	75.3334
DEL-WS7	2.00	37	18.50	2.00				
DEL WS8	2.00	35.5	17.75	2.00	20 seconds recovery time			
S Delta					2.8	4.31E-02	4.31E-04	37.2165
DEL-WS9	2.00	31.3	15.65	2.00				
DEL-WS10	2.00	32	16.00	2.00				
DEL-WS11	2.00	33	16.50	2.00				
DEL-WS12	2.00	32.5	16.25	2.00				
DEL-WD12	2.00	37	18.50	2.00				
DEL-WS13	2.00	31.5	15.75	2.00				
DEL-WS14	2.00	32.3	16.15	2.00				
DEL-WS15	2.00	37	18.50	2.00				
DEL-WS16	2.00	31	15.50	2.00				
DEL-WS17	2.00	36	18.00	2.00				

Table 13 Slug test calculations

Slug Test graphs for To

Piezometer	Reference head	Delta elevation	Well depth+ stick-up	Pre sampling depth to water	Pre-sampling head (cm) (H)	Post-sampling delta head	Post-sampling head (cm) (Ho)	Time (sec)	Recovery depth to water	Recovery head (cm) (h)	Time (min)	Time (sec)	Well depth+ stickup
Bank R													
R-WS1	384	6.4	578	480.5	-90.1	162.97	-253.07	0	501	-110.6	70	4200	578
R-WD1	384	0	642	353.7	30.3	234.28	-203.98	0	357	27	70	4200	642
R-WS2	384	199.9	644	571.1	12.8	213.90	-201.10	0	575	8.9	84	5040	644
R-WD2	384	167.9	743	539.2	12.7	234.28	-221.58	0	639	-87.1	83	4980	743
R-W3	384	-9.5	439	345.5	29.0	224.09	-195.09	0	345	29.5	94	5640	439
Bank N													
N-W1	535	57.4	569	389	203.4	203.72	-0.32	0					569
N-W2	535	65.6	504	382	218.6	191.50	27.10	0					504
N-W3	535	0	434	319.3	215.7	234.28	-18.58	0	318	217	90	5400	434
N-W4	535	27.4	418	210.6	351.8	234.28	117.52	0	211	351.4	65	3900	418
Bank H													
H-W1	292.9	0	408	271	21.9	229.18	-207.28	0	326	-33.1	235	14100	408
H-WS2	292.9	24.8	417	222	95.7	234.28	-138.58	0	277	40.7	225	13500	417
H-WD2	292.9	35.7	537	310	18.6	234.28	-215.68	0	313	15.6	218	13080	537
H-W3	292.9	23.6	427.7	339	-22.5	234.28	-256.78	0	355	-38.5	211	12660	427.7
Bank D													
D-W1	126.2	0	179	124	2.2	77.59	-75.39	0	NO DATA				179
D-W2	126.2	12.2	110	80	58.4	77.59	-19.19	0					110
D-W3	126.2	-7.2	191	124	-5.0	77.59	-82.59	0					191
N Delta													
DEL-WS1	88	0	159.5	88	0.0	79.58	-79.58		Rapid recovery - See previous page				159.5
DEL-WD1	88	-0.5	229.2	86	1.5	79.58	-78.08						229.2
DEL-WS2	82	0	178.5	82	0.0	79.58	-79.58						178.5
DEL-WS3	82	3.5	122.6	76	9.5	79.58	-70.08						122.6
DEL-WS4	82	7.2	179.9	78	11.2	79.58	-68.38						179.9
DEL-WS5	82	10	122	78	14.0	79.58	-65.58						122
DEL-WS6	82	24.7	194.5	91	15.7	79.58	-63.88						194.5
DEL-WS7	82	28.5	189.6	96	14.5	79.58	-65.08						189.6
DEL WS8	82	31.6	200.4	94	19.6	79.58	-59.98						200.4
S Delta													
DEL-WS9	77.5	0	126.2	70	7.5	79.58	-72.08						126.2
DEL-WS10	77.5	11.8	113.2	74	15.3	79.58	-64.28						113.2
DEL-WS11	77.5	5.1	183	64	18.6	79.58	-60.98						183
DEL-WS12	104	0	120.5	104	0.0	79.58	-79.58						120.5
DEL-WD12	104	-22.2	305	84	-2.2	79.58	-81.78						305
DEL-WS13	104	-1	164.3	106	-3.0	79.58	-82.58						164.3
DEL-WS14	104	-14.3	201.8	89	0.7	79.58	-78.88						201.8
DEL-WS15	84	0	204.8	84	0.0	79.58	-79.58						204.8
DEL-WS16	?		215										215
DEL-WS17	?		223.4	136		79.58							223.4

Peizometers	(H-h)	(H-Ho)	(H-h)/(H-Ho)	Time (sec)	log (H-h)/(H-Ho)
Bank R					
R-WS1	20.5	163.0	0.126	4200	-0.9
R-WD1	3.3	234.3	0.014	4200	-1.9
R-WS2	3.9	213.9	0.018	5040	-1.7
R-WD2	99.8	234.3	0.426	4980	-0.4
R-W3	0.0	224.1	0.000	5640	-4.4
Bank N					
N-W1					
N-W2					
N-W3	0.0	234.3	0.000	5400	-4.4
N-W4	0.4	234.3	0.002	3900	-2.8
Bank H					
H-W1	55.0	229.2	0.240	14100	-0.6
H-WS2	55.0	234.3	0.235	13500	-0.6
H-WD2	3.0	234.3	0.013	13080	-1.9
H-W3	16.0	234.3	0.068	12660	-1.2
Bank D					
D-W1	NO DATA				
D-W2					
D-W3					
N Delta					
DEL-WS1	Rapid recovery - See previous page				
DEL-WD1					
DEL-WS2					
DEL-WS3					
DEL-WS4					
DEL-WS5					
DEL-WS6					
DEL-WS7					
DEL WS8					
S Delta					
DEL-WS9					
DEL-WS10					
DEL-WS11					
DEL-WS12					
DEL-WD12					
DEL-WS13					
DEL-WS14					
DEL-WS15					
DEL-WS16					
DEL-WS17					

To=(H-h)/(H-Ho)

where:

H=initial head

Ho=initial drawdown

h=measured head

REFER TO FIGURE 19

boreholes. Since the average grain size of sediments appears to increase downstream, the general trend of increasing hydraulic conductivity values from the higher banks (K $\approx 1x10^{-6}$ m/s) to the lower banks and the delta (K $\approx 1x10^{-4}$ m/s) indicated by more rapid water level recovery rates is reasonable. The effective porosity of all sediments was estimated to be 35% (0.35), a value typical of many unconsolidated silt and sand-rich deposits (Selley 1976).

Groundwater levels were measured in each piezometer before sampling. Since these were measured relative to the nearest river or harbour surface-water level at the same time, the levels could be used to calculate horizontal and vertical hydraulic gradients between individual piezometers and between the piezometers and the river or harbour (figures 26 to 32).

Overall, groundwater flow in the sediment banks was towards the river. Horizontal hydraulic gradients in the sediment banks were lowest in Bank R (0.007 to 0.06 m/m towards the river, figure 26) and Bank D (0.006 to 0.02 m/m towards the river, figure 27), and highest in Bank N (0.06 to 0.14 m/m towards the river, figure 28) and Bank H (0.01 to 0.08 m/m towards the river, figure 29). Horizontal hydraulic gradients away from the river were measured in one piezometer in Bank R and one piezometer in Bank D. These piezometers were near the river bank and the hydraulic gradient reversal probably indicates a lag in water level response in the piezometer to changing river levels rather than indicating hydraulic conditions in the sediment banks in general.

Horizontal hydraulic gradients between the south lobe of the delta and the river ranged from 0.001 to 0.006 m/m towards the river (figure 30) indicating the potential for groundwater flow from the delta to the river. However, hydraulic gradients from the south lobe towards the harbour were very low and variable, ranging from $-1x10^{-3}$ to $1x10^{-4}$ m/m (figure 31) indicating only minimal potential for flow under these tidal conditions. Water levels in the transect of piezometers on the north lobe of the delta indicated that, under rising tide conditions, groundwater flow in the north lobe was still towards the harbour, with horizontal hydraulic gradients typically in the 0.001 to 0.003 m/m range. Under conditions in the field, water at the harbour/delta interface was often largely fresh (ie river water with relatively low EC values), and therefore the density differences due to saline harbour water are likely to be minimal.

Approaches to modelling

Two approaches were used to calculate groundwater flow rates and chemical fluxes within the saturated zone of the sediment banks and delta to the King River and Macquarie Harbour. These approaches included 1-dimensional steady-state groundwater flow modelling based on Darcy's Law and 2-dimensional steady-state groundwater flow and solute transport modelling using the numerical model FLOTRANS (Guiger et al 1995).

Darcy flow modelling

The 1-D form of Darcy's Law (equation 1) was used to estimate the Darcy flux from sediment banks R, N, H, and D to the King River (figures 26 to 29), from the south lobe of the delta to the King River (figure 30) and from the north and south lobes of the delta to Macquarie Harbour (figures 31 and 32).

$$q_l = -K\frac{dh}{dl} \qquad \text{Equation 1}$$

where q_l = Darcy flux or specific discharge (m/s); K = hydraulic conductivity (m/s); and dh/dl = hydraulic gradient (m/m), where l = x (horizontal gradient) or l = y (vertical gradient)

Hydraulic conductivity values measured or estimated from water level responses (table 12) were used as field-measured hydraulic gradients (figures 26 to 32). For Banks R, N, H and D, the resulting Darcy flux values were used to estimate water fluxes from the sediment banks into the river across a 1 m wide (bank length) by 2 m long (river bottom) discharge face (figures 26 to 30). A discharge face of 1 m wide by 1 m long was assumed for the contact of the King River and Macquarie Harbour with the delta.

The average linear velocity of groundwater between individual wells and between the banks or delta and the harbour was estimated using equation 2. These values could then be used to estimate travel times of groundwater within the sediment banks and delta.

$$\bar{v}_l = \frac{q_l}{n} \qquad \text{Equation 2}$$

where $\bar{v}_l$ = average linear velocity of groundwater (m/s); q_l = Darcy flux or specific discharge (m/s); n = effective porosity

Two-dimensional steady-state groundwater flow and solute transport modelling

The numerical model FLOTRANS (Guiger et al 1995) was used to model 2-dimensional, cross-sectional, steady-state groundwater flow and solute-transport between Bank H and the river and between the south lobe of the delta and the river. The model is based on the following 2-D groundwater flow equation (equation. 3) and the 2-D advection dispersion equation (equation. 4).

$$\frac{\partial h}{\partial x}\left(K_{xx}\frac{\partial h}{\partial x}\right) + \frac{\partial h}{\partial y}\left(K_{yy}\frac{\partial h}{\partial y}\right) = 0 \qquad \text{Equation 3}$$

$$\frac{D_{xx}}{R}\frac{\partial^2 C}{\partial x^2} + \frac{D_{yy}}{R}\frac{\partial^2 C}{\partial y^2} - \frac{\bar{v}_{xx}}{R}\frac{\partial C}{\partial x} - \frac{\bar{v}_{yy}}{R}\frac{\partial C}{\partial y} = \frac{\partial C}{\partial t} \qquad \text{Equation 4}$$

where: K_{xx} = horizontal hydraulic conductivity (m/s); K_{yy} = vertical horizontal hydraulic conductivity (m/s); R = retardation factor (1 + (ρb/n) K_d); h = hydraulic head (m); C = solute concentration in groundwater (g/m^3 = mg/L); D_{xx} = hydrodynamic dispersion coefficient (parallel to x) (m^2/s); D_{yy} = hydrodynamic dispersion coefficient (parallel to y) (m^2/s); $\bar{v}_{xx}$ = average horizontal linear velocity of groundwater (m/s); $\bar{v}_{yy}$ = average vertical linear velocity of groundwater (m/s); n = effective porosity; ρb = bulk density of saturated porous medium (g/m^3); and Kd = distribution coefficient (solid vs aqueous concentration)

Similar boundary conditions were used for each of the problems modelled with FLOTRANS. In each case, the boundary furthest from the river was assumed to be a no-flow boundary, as was the base of the modelled domain. The top of the model domain was defined as a constant flux boundary, with a recharge rate of 0.002 m/d, approximately 20% of annual precipitation. The boundary at the contact between surface water and groundwater was a constant head boundary extending for 1 or 2 m into the King River.

In each case, hydraulic conductivity was assumed to be isotropic and homogeneous within the domain. Initially these values were based on field estimates but they were later refined during calibration and sensitivity analyses. Sensitivity analyses were performed in conjunction with calibration steps primarily to determine the effects of varying hydraulic conductivity values and recharge rates on the resulting configuration of the water table.

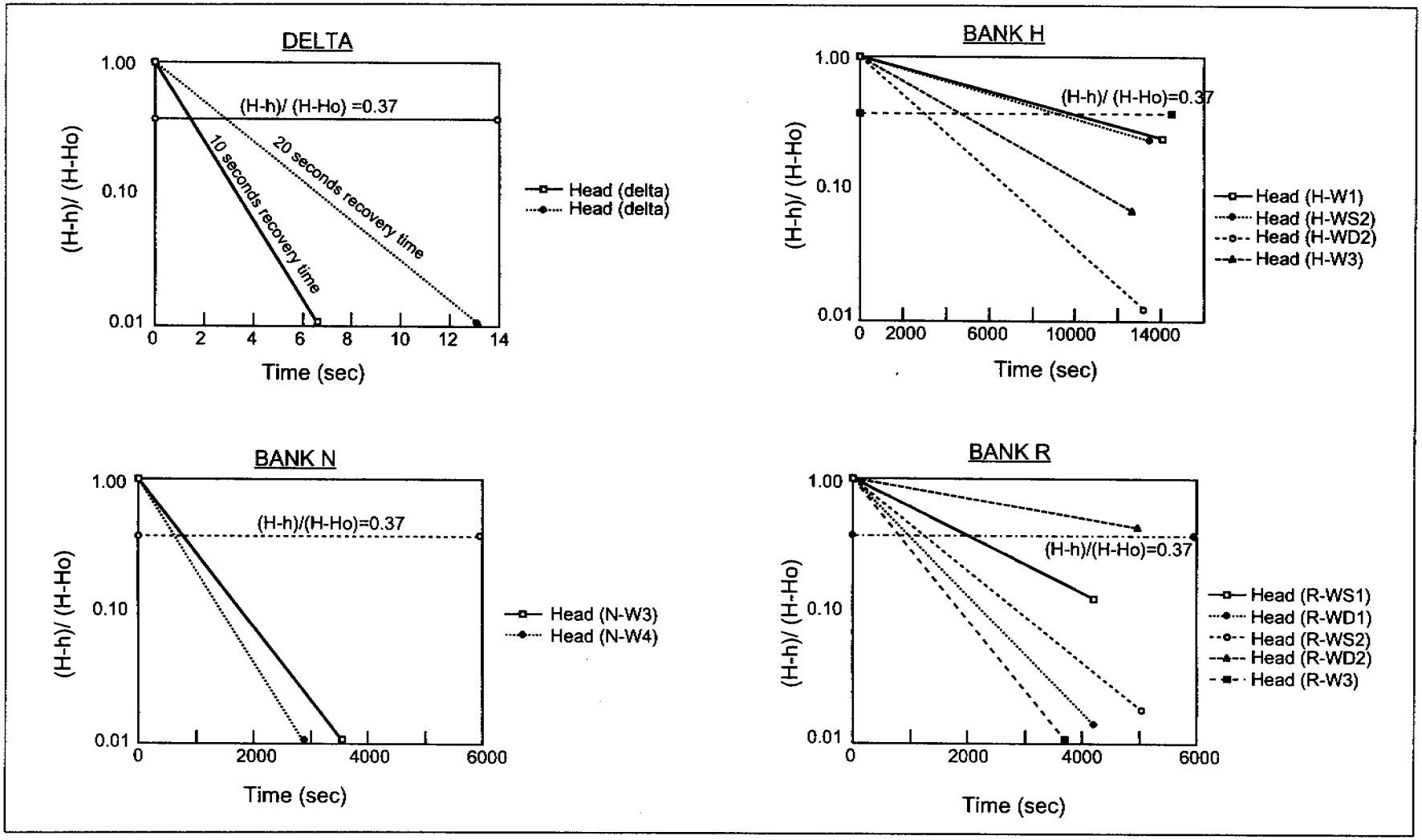

Figure 25 Graphical analysis of hydraulic head for the delta and banks

Geometric mean K (av) = 3.29E-07 m/sec

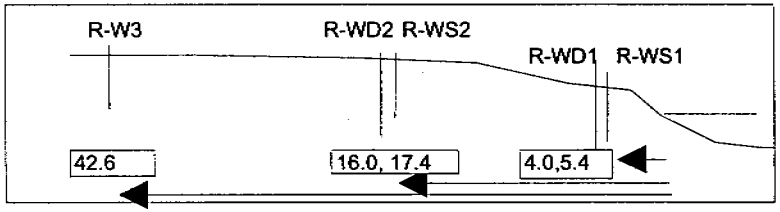

Piezometer	Reference head (cm)	Delta elevation (cm)	Well depth+ stickup (cm)	Pre sampling depth to water (cm)	Pre-sampling head (cm)	Screen elevation (middle) (cm)
R-WS1	384	6.4	578	480.5	-90.1	-165
R-WD1	384	0	642	353.7	30.3	-235
R-WS2	384	199.9	644	571.1	12.8	-45
R-WD2	384	167.9	743	539.2	12.7	-175
R-W3	384	-9.5	439	345.5	29.0	-100

Horizontal Hydraulic Gradients	m/m	wrt river	K (m/s) (minimum)	Darcy flux (m/s)	Darcy flux (m/d)	Assumed Porosity	Average linear velocity (m/s)	Average linear velocity (m/d)	Flux/2m deep, 1m wide (m3/d)	Flux/2m deep, 1m wide (l/d)
R-WS1 to river	-0.225	away	9.76E-08	-2.198E-08	-0.0018995	0.35	-6.281E-08	-0.005	-0.00380	-3.8
R-WD1 to river	0.056	towards	3.24E-07	1.818E-08	0.0015708	0.35	5.194E-08	0.004	0.00314	3.1
R-WS2 to river	0.008	towards	5.46E-07	4.368E-09	0.0003774	0.35	1.248E-08	0.001	0.00075	0.8
R-WD2 to river	0.007	towards	6.60E-07	4.817E-09	0.0004162	0.35	1.376E-08	0.001	0.00083	0.8
R-W3 to river	0.007	towards	1.00E-07	6.808E-10	5.882E-05	0.35	1.945E-09	0.000	0.00012	0.1

Vertical Hydraulic Gradients	m/m	
R-WD1 to R-WS1	-0.984	upward
R-WS2 to R-WD2	0.030	downward

Comments

R-WS1 to river: *lower K therefore likely lag time for response to river level changes*

Figure 26 Bank R – hydraulic gradient and fluxes

Geometric mean K (av) = 8.43E-07 m /sec

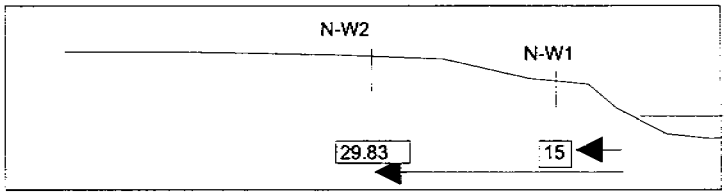

Piezometer	Reference head (cm)	Delta elevation (cm)	Well depth+ stickup (cm)	Pre sampling depth to water (cm)	Pre-sampling head (cm)	Screen elevation (middle) (cm)
N-W1	535	57.4	569	389	203.4	45
N-W2	535	65.6	504	382	218.6	105
N-W3	535	0	434	319.3	215.7	120
N-W4	535	27.4	418	210.6	351.8	155

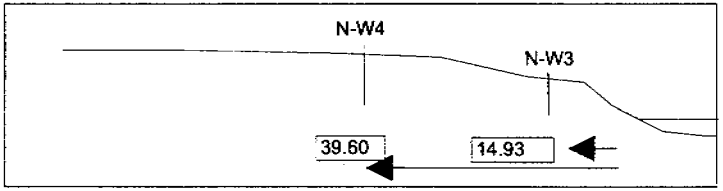

Horizontal Hydraulic Gradients	m/m	wrt river	K (m/s) (minimum)	Darcy flux (m/s)	Darcy flux (m/d)	Assumed porosity	Average linear velocity (m/s)	Average linear velocity (m/d)	Flux/2m deep, 1m wide (m3/d)	Flux/2m deep, 1m wide (l/d)
N-W1 to river	0.136	towards	8.43E-07	1.14336E-07	0.00987867	0.35	3.2668E-07	0.028	0.01976	**19.8**
N-W2 to river	0.073	towards	8.43E-07	6.17905E-08	0.0053387	0.35	1.7654E-07	0.015	0.01068	10.7
N-W3 to river	0.144	towards	7.24E-07	1.04599E-07	0.00903738	0.35	2.9886E-07	0.026	0.01807	**18.1**
N-W4 to river	0.089	towards	9.82E-07	8.72393E-08	0.00753747	0.35	2.4926E-07	0.022	0.01507	15.1
N-W2 to N-W1	0.010	towards	8.43E-07	8.64226E-09	0.00074669	0.35	2.4692E-08	0.002		
N-W4 to N-W3	0.055	towards	8.43E-07	4.65172E-08	0.00401909	0.35	1.3291E-07	0.011		

Hydraulic Gradients Parallel to Bank	m/m	wrt river direction	K (m/s) (minimum)	Darcy flux (m/s)	Darcy flux (m/d)	Assumed porosity	Average linear velocity (m/s)	Average linear velocity (m/d)
N-W3 to N-W1	0.001	down flow	8.43E-07	7.97787E-10	6.8929E-05	0.35	2.2794E-09	0.0002
N-W4 to N-W2	0.011	down flow	8.43E-07	8.87147E-09	0.00076649	0.35	2.5347E-08	0.0022

Figure 27 Bank D – hydraulic gradient and fluxes

Geometric mean K (av) = 1.1E-07 m/sec

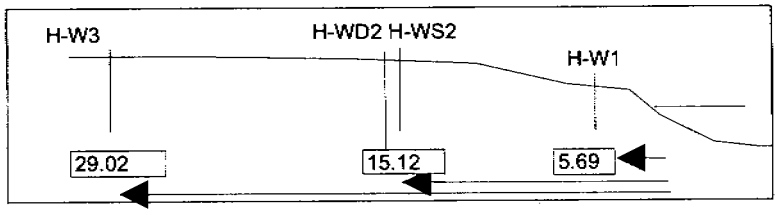

Piezometer	Reference head (cm)	Delta elevation (cm)	Well depth+ stickup (cm)	Pre sampling depth to water (cm)	Pre-sampling head (cm)	Screen elevation (middle) (cm)
H-W1	292.9	0	408	271	21.9	-100
H-WS2	292.9	24.8	417	222	95.7	-80
H-WD2	292.9	35.7	537	310	18.6	-200
H-W3	292.9	23.6	427.7	339	-22.5	-120

Horizontal Hydraulic Gradients	m/m	wrt river	K (m/s) minimum	Darcy flux (m/s)	Darcy flux (m/d)	Assumed porosity	Average linear velocity (m/s)	Average linear velocity (m/d)	Flux/2m deep, 1m wide (m3/d)	Flux/2m deep, 1m wide (l/d)
H-W1 to river	0.038	towards	6.67E-08	2.56719E-09	0.0002218	0.35	7.335E-09	0.0006	0.00044	0.4
H-WS2 to river	0.063	towards	7.18E-08	4.54448E-09	0.0003926	0.35	1.298E-08	0.0011	0.00079	0.8
H-WD2 to river	0.012	towards	1.44E-07	1.77143E-09	0.0001531	0.35	5.061E-09	0.0004	0.00031	0.3
H-W3 to river	-0.008	away	2.19E-07	-1.698E-09	-0.0001467	0.35	-4.851E-09	-0.0004	-0.00029	-0.3
H-W3 to H-WS2	-0.085	away	1.11E-07	-9.4269E-09	-0.0008145	0.35	-2.693E-08	-0.0023	-0.00163	-1.6
H-WS2 to H-WS1	0.078	towards	1.11E-07	8.67579E-09	0.0007496	0.35	2.479E-08	0.0021	0.00150	1.5

Vertical Hydraulic Gradients	m/m	
R-WS2 to R-WD2	0.802	downward

Comments

N.B.: Water level in R-WS2 appears to be "perched" (~70 cm) above bank water table

Figure 28 Bank N – hydraulic gradient and fluxes

Estimated K (av) = 1.00E-05 m/sec

(no data)

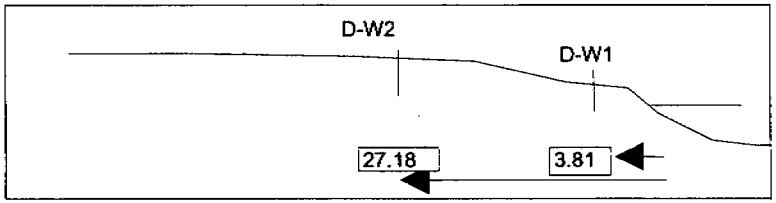

Piezometer	Reference head (cm)	Delta elevation (cm)	Well depth+ stickup (cm)	Pre sampling depth to water (cm)	Pre-sampling head (cm)	Screen elevation (middle) (cm)
D-W1	126.2	0	179	124	2.2	-25
D-W2	126.2	12.2	110	80	58.4	65
D-W3	126.2	-7.2	191	124	-5.0	-50

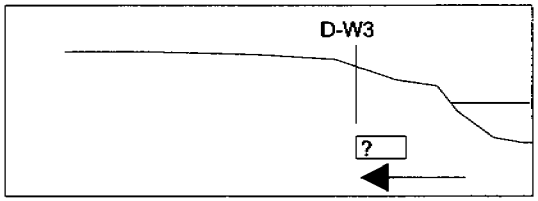

Horizontal Hydraulic Gradients	m/m	wrt river	K (m/s) (minimum)	Darcy flux (m/s)	Darcy flux (m/d)	Assumed porosity	Average linear velocity (m/s)	Average linear velocity (m/d)	Flux/2m deep, 1m wide (m3/d)	Flux/2m deep, 1m wide (l/d)
D-W1 to river	0.006	towards	1.00E-05	5.77428E-08	0.004989	0.35	1.65E-07	0.014	0.00998	**10.0**
D-W2 to river	0.021	towards	1.00E-05	2.14864E-07	0.0185642	0.35	6.139E-07	0.053	0.03713	37.1
D-W3 to river	-0.014	away	1.00E-05	-1.4286E-07	-0.0123429	0.35	-4.082E-07	-0.035	-0.02469	**-24.7**
D-W2 to D-W1	0.024	towards	1.00E-05	2.40479E-07	0.0207774	0.35	6.871E-07	0.059		

Hydraulic Gradients Parallel to Bank	m/m	wrt river direction	K (m/s) (minimum)	Darcy flux (m/s)	Darcy flux (m/d)	Assumed porosity	Average linear velocity (m/s)	Average linear velocity (m/d)
D-W3 to D-W1	-0.001	up flow	1.00E-05	-1.4487E-08	-0.0012517	0.35	-4.139E-08	-0.004

Figure 29 Bank H – hydraulic gradient and fluxes

Solute transport modelling in Bank H and the south lobe of the delta perpendicular to the King River was based on the final 'best-fit' 2-D groundwater flow models (Appendix 6, figures A6.1, A6.5). In both cases, a constant concentration of solute (50 mg/L) was maintained at the water table boundary and the solute was assumed to behave conservatively within the flow system (ie non reactive, retardation factor (R) = 1). The initial solute concentration in the domain was set at 0 mg/L. The solute transport models for Bank H were run for 4000 days, and 1000 days for the south lobe. Results of the 2-D groundwater flow and solute transport modelling are included in Appendix 6.

For both Bank H and the south lobe, the groundwater flow models were relatively insensitive to varying recharge rates from about 10 to 50% of precipitation, however, the best fit for both models was found with a recharge rate of 0.002 m/d. The recharge rate was assumed to be constant between the banks and the delta. The flow models were, however, extremely sensitive to variations in hydraulic conductivity.

Bank H

Using the average of the field measured values for hydraulic conductivity in Bank H ($K = 10^{7}$ m/s), the water table rose several metres over measured hydraulic head values. Only when hydraulic conductivity was increased to about $5x10^{-6}$ m/s was the mounding of the water table minimised, and hydraulic head values close to those measured in the field were reproduced (Appendix 6, figure A6.1). The increased value for hydraulic conductivity is not difficult to reconcile if we consider that smearing of clays may have occurred during borehole drilling. However, it does indicate that hydraulic conductivity values for the high sediment banks (Banks R, N and H) are probably about an order of magnitude greater than those calculated from the 1-D Darcy Flow modelling (figures 26, 28 and 29).

Fluxes from Bank H to the river, calculated from the 2-D groundwater flow model, are on the order of 40 L/d/linear m of sediment bank (Appendix 6, figure A6.2). As in the 1-D Darcy flux model, discharge was assumed to occur over a discharge face of 2 m^2. Fluxes from the 2-D modelling are about 2 orders of magnitude greater than those calculated from the simple 1-D Darcy flux model (≈0.5 L/d), however, if the calculated Darcy fluxes are corrected to account for the higher hydraulic conductivity of the sediment bank, the fluxes from the 1-D (25 L/d) and 2-D modelling (40 L/d) are similar.

The average linear groundwater velocity calculated from the 2-D modelling was $9.7x10^{-2}$ m/d in Bank H (Appendix 6, figure A6.3). Based on this value, the average residence time of groundwater with a 15 m travel path through the saturated zone would be on the order of 6 months and that with a 30 m travel path would be over 1 year.

Solute transport modelling for Bank H indicates that solute concentrations near to the river edge (eg in piezometer H-W1) would attain steady state conditions after about 1 to 1.5 yr (Appendix 6, figure A6.4) and that it would take only a month or two after entering the groundwater flow system for a conservative solute to begin discharging to the river.

South lobe of delta – perpendicular to the King River

In the south lobe of the delta, the estimated hydraulic conductivity value of $1x10^{-4}$ m/s (12 m/d) and the assumed recharge rate of 0.002 m/d produced a reasonable fit to the hydraulic head measured in the piezometers perpendicular to the King River (Appendix 6, figure A6.5).

Fluxes from the south lobe of the delta to the river, calculated from the 2-D groundwater flow model, are in the order of 100 L/d per linear m of delta/river interface (Appendix 6,

Estimated K (av) = 1.00E-04 m/sec

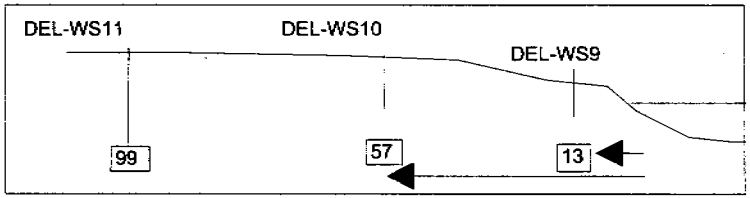

Piezometer	Reference head (cm)	Delta elevation (cm)	Well depth+ stickup (cm)	Pre sampling depth to water (cm)	Pre-sampling head (cm)	Screen elevation (middle) (cm)
DEL-WS9	77.5	0	126.2	70	7.5	-26
DEL-WS10	77.5	11.8	113.2	74	15.3	-5
DEL-WS11	77.5	5.1	183	64	18.6	-77

Horizontal Hydraulic Gradients	m/m	wrt river	K (m/s) (minimum)	Darcy flux (m/s)	Darcy flux (m/d)	Assumed porosity	Average linear velocity (m/s)	Average linear velocity (m/d)	Flux/1m deep, 1m wide (m3/d)	Flux/1m deep, 1m wide (l/d)
DEL-WS9 to river	0.006	towards	1.00E-04	5.76923E-07	0.0498462	0.35	1.648E-06	0.14	0.04985	49.8
DEL-WS10 to river	0.003	towards	1.00E-04	2.68421E-07	0.0231916	0.35	7.669E-07	0.07	0.02319	23.2
DEL-WS11 to river	0.002	towards	1.00E-04	1.87879E-07	0.0162327	0.35	5.368E-07	0.05	0.01623	16.2
DEL-WS10 to DEL-WS9	0.002	towards	1.00E-04	1.77273E-07	0.0153164	0.35	5.065E-07	0.04		
DEL-WS11 to DEL-WS9	0.001	away	1.00E-04	1.12121E-07	0.0096873	0.35	3.203E-07	0.03		

Comments: Tide level rising during measurements

Figure 30 South lobe of delta – hydraulic gradient and fluxes perpendicular to King River

Estimated K (av) = 1.00E-04 m/sec

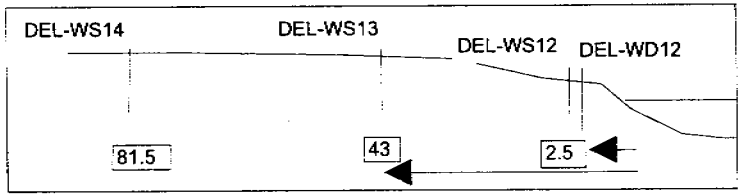

Piezometer	Reference head (cm)	Delta elevation (cm)	Well depth+ stickup (cm)	Pre sampling depth to water (cm)	Pre-sampling head (cm)	Screen elevation (middle) (cm)
DEL-WS12	104	0	120.5	104	0.0	-50
DEL-WD12	104	-22.2	305	84	-2.2	-205
DEL-WS13	104	-1	164.3	106	-3.0	-45
DEL-WS14	104	-14.3	201.8	89	0.7	-98

Horizontal Hydraulic Gradients	m/m	wrt harbour	K (m/s) (minimum)	Darcy flux (m/s)	Darcy flux (m/d)	Assumed porosity	Average linear velocity (m/s)	Average linear velocity (m/d)	Flux/1m deep, 1m wide (m3/d)	Flux/1m deep, 1m wide (l/d)
DEL-WS12 to harbour	0.0000	none	1.00E-04	0	0	0.35	0	0	0.00000	0.00
DEL-WD12 to harbour	-0.0088	away	1.00E-04	-8.8E-07	-0.076032	0.35	-2.514E-06	-0.217	-0.07603	-76.0
DEL-WS13 to harbour	-0.0007	away	1.00E-04	-6.9767E-08	-0.0060279	0.35	-1.993E-07	-0.017	-0.00603	-6.0
DEL-WS14 to harbour	0.0001	towards	1.00E-04	8.58896E-09	0.0007421	0.35	2.454E-08	0.002	0.00074	0.7
DEL-WS13 to DEL-WS12	-0.0007	away	1.00E-04	-7.4074E-08	-0.0064	0.35	-2.116E-07	-0.018		
DEL-WS14 to DEL-WS12	0.0001	towards	1.00E-04	8.86076E-09	0.0007656	0.35	2.532E-08	0.002		

Comments: Tide level rising during measurements

Figure 31 South lobe of delta – hydraulic gradient and fluxes perpendicular to Macquarie Harbour

Estimated K (av) =1.00E-04 m/sec

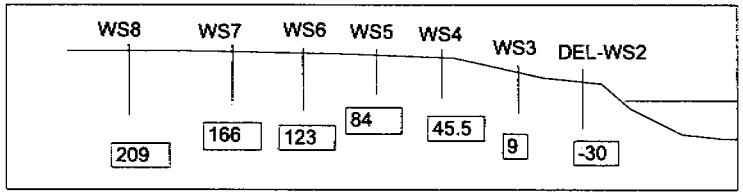

Piezometers	Reference head (cm)	Delta elevation (cm)	Well depth+ stickup (cm)	Pre sampling depth to water (cm)	Pre-sampling head (cm)	Screen elevation (middle) (cm)
DEL-WS2	82	0	178.5	82	0.0	-80
DEL-WS3	82	3.5	122.6	76	9.5	-20
DEL-WS4	82	7.2	179.9	78	11.2	-70
DEL-WS5	82	10	122	78	14.0	-15
DEL-WS6	82	24.7	194.5	91	15.7	-70
DEL-WS7	82	28.5	189.6	96	14.5	-65
DEL WS8	82	31.6	200.4	94	19.6	-70

Horizontal Hydraulic Gradients	m/m	wrt harbour	K (m/s) (minimum)	Darcy flux (m/s)	Darcy flux (m/d)	Porosity (0-1)	Average linear velocity (m/s)	Average linear velocity (m/d)	Flux/1m deep, 1m wide (m3/d)	Flux/1m deep, 1m wide (l/d)
DEL-WS2 to harbour	0.0000	none	1.00E-04	0	0	0.35	0	0.00	0.00000	0.0
DEL-WS3 to harbour	0.0106	towards	1.00E-04	1.05556E-06	0.0912	0.35	3.016E-06	0.26	0.09120	91.2
DEL-WS4 to harbour	0.0025	towards	1.00E-04	2.46154E-07	0.0212677	0.35	7.033E-07	0.06	0.02127	21.3
DEL-WS5 to harbour	0.0017	towards	1.00E-04	1.66667E-07	0.0144	0.35	4.762E-07	0.04	0.01440	14.4
DEL-WS6 to harbour	0.0013	towards	1.00E-04	1.27642E-07	0.0110283	0.35	3.647E-07	0.03	0.01103	11.0
DEL-WS7 to harbour	0.0009	towards	1.00E-04	8.73494E-08	0.007547	0.35	2.496E-07	0.02	0.00755	7.5
DEL-WS8 to harbour	0.0009	towards	1.00E-04	9.37799E-08	0.0081026	0.35	2.679E-07	0.02	0.00810	8.1

Figure 32 North lobe of delta – hydraulic gradient and fluxes perpendicular to Macquarie Harbour

figure A6.6). Discharge in the 2-D model was assumed to occur over a discharge face of 5 m^2 whereas discharge in the Darcy flux model was assumed to occur over 1 m^2. Fluxes calculated from the 1-D Darcy flux model ranged from about 20 to 50 L/d, which if taken over a 5 m^2 discharge area would range from 100 to 250 L/d. Again, the fluxes calculated from the 1-D and 2-D modelling are similar and indicate significant discharge from the delta to the river under the conditions present during monitoring.

The average linear groundwater velocity calculated from the 2-D modelling was 8.1×10^{-2} m/d in the south lobe of the delta (Appendix 6, figure A6.7). Based on this value, the average residence time of groundwater with a 50 m travel path through the saturated zone would be in the order of 2 years and that with a 100 m travel path would be at least 3 to 5 years.

Solute transport modelling indicates that solute concentrations at a piezometer located in the delta about 15 m from the river bank (eg DEL-WS9) would attain steady state conditions after about 1.5 to 2 years (Appendix 6, figure A6.8) whereas concentrations about 60 m from the river bank would take about 2.5 to 3 years to reach steady state conditions.

Conclusions from hydrogeological modelling

The major conclusions drawn from the 1-D and 2-D groundwater flow modelling and the 2-D solute transport modelling are:

- Calculated hydraulic conductivity values in the higher banks (Banks R, N, and H) are probably 10 to 50 times too low. This is most probably due to smearing of clays in the sediments during piezometer installation. More realistic hydraulic conductivity values for these sediments banks are likely to be in the order of 10^{-6}m/s.
- Hydraulic conductivity values are higher in the lowest sediment bank (Bank D) and the north and south lobes of the delta. Based on water level recovery times, the hydraulic conductivity of these sediments is likely to be in the order of 10^{-4} m/s.
- Groundwater flux from Bank H to the King River is estimated to be between 25 and 40 L/d/linear m. The discharge face was assumed to extend 2 m into the King River. It is considered likely that groundwater fluxes from Banks N and R, and intervening banks, would be similar to those determined for Bank H.
- Groundwater flux from the south lobe of the delta to the King River is estimated to be between 100 and 250 L/d/linear m over a discharge face assumed to extend 5 m under water. This area may be excessive, and groundwater discharge to the river would decline proportionally as the discharge face is reduced. If the discharge face extended only 1 m under water, the fluxes would be in the order of 20 to 50 L/d/linear m.
- Groundwater fluxes from the delta to the harbour were estimated only from the 1-D Darcy Flux modelling. The calculated fluxes were highly variable because of the large range of hydraulic gradients measured along the north and south lobe transects. For the north lobe of the delta, fluxes ranged from 10 to 90 L/d/m^2into the harbour, whereas in the south lobe, hydraulic gradients indicated that water during some periods of the high tide was flowing into the delta from the harbour at fluxes of up to 70 L/d/m^2.

All of the modelling results presented above assume steady state conditions, however, water levels in the King River and Macquarie Harbour fluctuate significantly in response to John Butters Power Station requirements and storm and tidal influences. Therefore, the calculated fluxes are only valid for the conditions at the time of monitoring, but they indicate that there is the potential for significant groundwater flow to occur from the sediment banks and the delta to the King River and Macquarie Harbour. These fluxes provide the basis from which to

estimate loading of contaminants from the tailings-rich sediments to these water bodies. Detailed monitoring to provide time-series data showing the response of hydraulic head in the sediment banks and delta to changing river and harbour levels throughout the year would be required to calculate groundwater fluxes under different hydraulic conditions.

6.2 Geochemistry

Introduction

The geochemistry of the groundwater and sediment was modelled to:

- test the quality of the analytical data for groundwater samples;
- identify the predominant aqueous species in the groundwater;
- predict the saturation states of minerals; and
- provide insight into whether equilibrium models are sufficient to model the interaction between sediment and groundwater in the banks and delta.

The modelling package chosen was MINTEQA2 and it was used to calculate distributions of aqueous species and mineral saturation indices using the measured groundwater compositions. MINTEQA2 was chosen over others (eg EQ3NR/EQ6, SOLVEQ/CHILLER, THERMO) because it has a more extensive database of mineral and aqueous species likely to be important in sulphidic mine tailings. MINTEQA2 is a combination of the programs MINEQL (mathematical methods and computer code) and WATEQ (database of thermodynamic properties for mineral, aqueous and gaseous species). It was developed by the United States Environmental Protection Agency and IBM-PC versions are freely available on the World Wide Web (http://www.epa.gov/gils/records/access/eta).

Several parameters are necessary to run the program. Temperature was input as 10°C for all runs because the ambient temperature during sampling in the field was usually 9 to 11°C. Input values of pH and Eh were those measured in the field for each sample. Element or aqueous species concentrations in mg/L were input after adjusting for dilution during acidification and recalculation to species appropriate for MINTEQA2 (eg As is input as H_3AsO_3 and/or H_3AsO_4). There are many options available with MINTEQA2; however, the most straightforward calculations were chosen in order to be able to interpret the results more reliably. Ionic strength was calculated from the modelled distribution of species, inorganic carbon (alkalinity) was not specified, mineral species were not allowed to react (dissolve, precipitate, adsorb/desorb) in any of the model calculations and the Davies equation (Stumm & Morgan 1981) was used to estimate activity coefficients for aqueous species. It was necessary to specify redox couples for elements with variable valence states, so the program would include all appropriate minerals and aqueous species in its calculations. This was problematic in some cases as the program would not always converge within the maximum number of iterations (200). Nitrogen and vanadium were problem elements. Co-, Sn-, Mo- and La-bearing species are not present in the MINTEQA2 database. Adsorption models were not included because of time constraints and the results of the leach tests provide evidence that adsorption is negligible in the sediment analysed.

Calculations were made for most of the analysed groundwater samples, except for a few that lacked field-measured pH and Eh. For each sample, a distribution of aqueous species and mineral saturation indices for all minerals within the database were calculated. An example output file is shown in Appendix 7. The results are summarised below.

Quality of the analytical data for groundwater samples

The quality of the analytical data was tested by calculating charge balances from the measured groundwater compositions and calculated distribution of species. The charge balance is expressed as:

$$\left[\frac{\sum \text{anions} - \sum \text{cations}}{\sum \text{anions} + \sum \text{cations}}\right] \times 100$$

Equation 5

In all cases, there was a calculated excess negative charge, ranging from <1 to 89%. There is no obvious reason for the excess of anions; however, there is a rough correlation with measured sulphate concentration and pH. Large charge imbalances are usually associated with high sulphate concentrations and low pH.

The most likely source of uncertainty is the sulphate concentrations. The other major anion, chloride, was reanalysed by Amdel after initial calculations showed charge imbalances. The results for chloride (table 3) are considered to be reliable. Measured metal concentrations in unacidified and acidified, filtered samples were usually similar, also indicating reliability. Errors in the concentrations of major cations (Na, K, Ca and Mg) are unlikely to be high enough, up to an order of magnitude, to explain charge imbalances. The sulphur concentrations are given in terms of sulphate, and it is possible that the sulphur existed as species with other valence states (eg S(IV), S(-II)). Calculations were made using Eh measured in the field. If the actual values were lower, thus more reduced conditions, or the groundwater were not at equilibrium, then it is possible that some of the sulphur was present as sulphite or sulphide, leading to improved charge balances. The amount of sulphate necessary to be present as sulphide to give charge balance was calculated to be <1 to ≈95%, depending on the sample.

Predominant aqueous species

Metals can exist in water as many aqueous species and the type(s) of species can affect mineral solubility, adsorption/desorption behaviour and possible bioavailability. The predicted predominant aqueous species are listed below for the metals measured and detected

in the groundwater samples. The species included in the database are listed in brackets after each element. Only a selected set of elements are discussed.

Aluminium

(Al^{3+}, $Al(OH)^{2+}$, $Al(OH)_2^{+}$, $Al(OH)_3(aq)$, $Al(OH)_4^{-}$, $Al(SO_4)^{+}$, $Al(SO_4)_2^{-}$)

The predicted predominant aqueous species of aluminium depend on pH and sulphate concentration. The aluminium hydroxide species are predicted to predominate in most cases, except for high sulphate concentration, low pH samples such as in Bank D, where about 80% of the aqueous aluminium is present as Al-sulphate species.

Arsenic

($H_4AsO_3^{+}$, $H_3AsO_3(aq)$, $H_2AsO_3^{-}$, $HAsO_3^{2-}$, AsO_3^{3-}, $H_3AsO_4(aq)$, $H_2AsO_4^{-}$, $HAsO_4^{2-}$, AsO_4^{3-})

In the north lobe of the delta samples the predominant aqueous species is predicted to $H_3AsO_3(aq)$; however, in the Banks D, H, N and R, and the more oxidised samples of the south lobe of the delta, the predominant species is $H_2AsO_4^{-}$ or in some cases near equal concentrations of reduced and oxidised arsenic species.

Cadmium

(Cd^{2+}, Cd-chlorides, Cd-hydroxides, Cd-sulphates, Cd-sulphides)

The speciation of cadmium is dependent on pH, chlorinity and sulphate, sulphide and total cadmium concentrations. No one species of cadmium is predicted to predominate over all samples. Mixtures of Cd^{2+}, Cd-chloride and Cd-sulphate species are predicted to be present, depending on the sample.

Chromium

(Cr^{2+}, Cr^{3+}, Cr-hydroxides, Cr-chlorides, Cr-sulphates, Cr-nitrate, Na-chromate)

Chromium was not detected in many samples, though when detected most were unfiltered and unacidified. In sample 3 from Bank D (D-W3; filtered and acidified), the highest measured Eh, the predominant chromium species was predicted to be Cr^{3+}.

Cobalt

(Co^{2+}, $Co(OH)^{+}$, Co^{3+})

Cobalt species are not included in the MINTEQA2 database; however, calculations with EQ3NR for sample DEL-WS9 predict that Co^{2+} is the predominant aqueous species.

Copper

(Cu^{+}, Cu^{2+}, Cu(I)-chlorides, Cu(II)-chlorides, - hydroxides, -sulphate, -bisulphide)

The speciation of aqueous copper is controlled by pH, redox, chlorinity, sulphate, sulphide and total copper concentrations. Copper was not detected in the groundwater samples from the north lobe of the delta. The predominant copper species predicted in the groundwater samples from the south lobe of the delta are mostly Cu^{2+} and $CuSO_4(aq)$, although in sample DEL-WS17 $CuCl_2^{-}$ and Cu^{+} were predicted to predominate. In all of the copper-containing samples from the sediment banks D, H, N and R Cu^{2+} and $CuSO_4(aq)$ were predicted to predominate, although Cu^{+} may be an important aqueous copper species in the more reduced samples (eg Bank N, sample N-W2).

Iron

(Fe^{2+}, Fe^{3+}, Fe(II)-sulphides and Fe(II)- and Fe(III)-chlorides, -hydroxides, and -sulphates)

Despite the many possible aqueous species for iron, the predominant ones were invariably predicted to be Fe^{2+} and $FeSO_4(aq)$, for both north and south lobes of the delta and all banks studied.

Lead

(Pb^{2+}, Pb-chlorides, -sulphides, -sulphates)

Aqueous lead is predicted to be distributed amongst several species, but Pb^{2+} and $PbSO_4(aq)$ made up more than 50% of the total lead in all samples.

Mercury

(Hg^{+}, Hg_4^{2+}, Hg-chlorides, -hydroxides, -sulphides and -sulphate)

Mercury concentrations were measured in 7 samples and detected in 4: north lobe of the delta (sample DEL-WS9), south lobe of the delta (sample DEL-WS14), Bank D (sample D-W3)

and Bank R (sample R-WD1). In all samples Hg(aq) was predicted to predominate, although in the sample from Bank D, $HgCl_2(aq)$ may be important.

Selenium

(HSe^-, $HSeO_3^-$, SeO_4^{2-}, Se(-II)-, Se(IV)- and Se(VI)-metal species, as well as protonated and deprotonated derivatives of the non-metal species)

Selenium concentrations were measured in 7 samples, and detected in 5. In a sample from the north lobe of the delta (sample DEL-WS2), HSe^- was the predominant species, but in all other samples from the north and south lobe of the delta and Bank H, $HSeO_3^-$ was predicted to be the predominant species.

Zinc

(Zn^{2+}, Zn-chlorides, -hydroxides, -bisulphides, -sulphates, -bicarbonates, -selenate)

In all samples, Zn^{2+} and Zn-sulphate species were predicted to predominate, with the exception of sample DEL-WS2 (north lobe of the delta), in which Zn^{2+} and $ZnCl^+$ were predicted to predominate.

Mineral saturation states

Mineral saturation states were calculated as part of the output from MINTEQA2. They are useful for indicating what minerals might be dissolving or precipitating into or from the groundwater, or controlling the groundwater composition. The calculations are based on an equilibrium model, so the results are only an indication, as kinetic factors may inhibit approach to equilibrium.

North lobe of the delta

The minerals which are commonly close to saturation (saturation index (SI) = log (Q/K) = -1 to 1) are: $Al(OH)_3$ (amorphous), chalcedony, cristobalite, hydrapatite (in P-bearing groundwater), amorphous silica, vivianite (Fe-phosphate), $ZnSiO_3$, wairakite, goethite/lepidocrocite, calcite/magnesite (in carbonate-bearing groundwater), talc, leucite, celestite, gypsum/anhydrite, Fe-vanadate and SbO_2 (in Sb-bearing groundwater).

The minerals which are commonly supersaturated (SI > 1) are: barium, Ba-arsenate, ferrous-hydroxychloride, magnetite/hematite, cuprous-ferrite, quartz, aluminium-hydroxysulphate, alunite, diaspore, halloysite, leonhardite, albite/K-feldspar, pyrophyllite, muscovite, laumontite, montmorillonite and Na-, K-, Mg- and Ca-nontronite. In particular, the nontronite minerals were usually supersaturated by 10 to 20 orders of magnitude ($10 < SI < 20$). In addition, some of the clay minerals (eg halloysite, leonhardite, muscovite (sericite), pyrophyllite, laumontite) were also predicted to be supersaturated by up to 10 orders of magnitude or more. The sulphate-bearing minerals may not be supersaturated, or at least as much as predicted, due to the uncertainty in the predicted concentrations/activities of sulphate aqueous species.

South lobe of the delta

In the south lobe of the delta, the minerals which are close to saturation ($-1 < SI < 1$) are: aluminium hydroxysulphate, boehmite, goethite/lepidocrocite, iron hydroxychloride, gypsum, amorphous silica, selenium metal (in Se-bearing groundwater), Fe-vanadate, and in some cases, gibbsite, diaspore, anhydrite, albite, laumontite, cuprite, cupricferrite, barium arsenate. The biggest difference relative to the samples from the north lobe of the delta is that aluminium-bearing minerals were less saturated/supersaturated in the south lobe of the delta.

The minerals predicted to be supersaturated were similar to those predicted in the north lobe of the delta. The most supersaturated minerals were the nontronite and clay minerals. Other silicates, eg feldspar, were in general undersaturated.

Bank D

The predicted saturated and supersaturated minerals are much the same as in the south lobe of the delta. The magnitude of saturation is much less (up to 10 log units for the nontronite species), with Fe-bearing, clay and other silicate minerals being less supersaturated or undersaturated. Cuprous ferrite is near saturation and cupric ferrite is well undersaturated, in contrast to the copper-bearing groundwater of the delta. The sampled groundwater was all unsaturated with respect to goethite/lepidocrocite, again in contrast to the delta groundwater. This reflects the much lower pH readings (2.5 to 3.0) in Bank D, compared with those measured in the delta ($5.5 < pH < 7.1$).

Bank H

Predictions of mineral saturation indices were similar to Bank D, except for copper-sulphide minerals which were close to saturation or supersaturated. Sample H-WS2 had a higher pH (5.7) than the other 3 samples from Bank H, and this is reflected in aluminium-bearing minerals being saturated to supersaturated.

Bank N

Sample N-W1 was predicted to be supersaturated with many Al-, Fe- and Cu-bearing minerals, but the other 3 groundwater samples from Bank N were similar with respect to mineral saturation as samples from Banks D and H.

Bank R

Most minerals were predicted to be undersaturated in the groundwater samples from Bank R. Exceptions were cuprous ferrite, barite, nontronite minerals and pyrophyllite.

To summarise, the groundwater in the banks were unsaturated or less supersaturated with respect to many minerals, compared with the groundwater in the delta. The low profile banks (D and H) were closer to the delta groundwater than those of the high profile river banks (N and R). The most likely reason for the differences is the groundwater in the banks is normally more acid and oxidised.

Controls on groundwater composition

The modelling indicates that groundwater compositions are controlled by a complex set of minerals and processes. Some elements appear to be controlled by mineral solubilities and equilibrium processes, while others are controlled either by unknown minerals or kinetic reactions.

There are two elements that may be controlled by mineral solubilities and equilibrium processes: Si and Fe. Both elements may not be directly important to water quality, but they can affect the precipitation or dissolution of other more toxic elements, eg Cu incorporated into copper-iron minerals and Al incorporated into aluminium-silicate minerals. Aqueous silica is predicted to be close to saturation with amorphous silica. This is consistent with petrographic observations of microcrystalline silica in many sediment samples. Aqueous iron in many samples is close to saturation with goethite/lepidocrocite. One of these phases likely comprises much of the iron coatings observed on detrital mineral grains. Other iron-bearing minerals are either supersaturated or undersaturated, eg magnetite and hematite are predicted to be supersaturated and pyrite and other iron sulphides are highly undersaturated. The iron sulphides may not be so undersaturated if the model estimates of aqueous sulphide/sulphate ratios are too low or the measured redox potentials (Eh) are too high.

Many elements are supersaturated with respect to one or more minerals. Groundwater is predicted to be supersaturated with respect to copper, with a cuprous ferrite solid phase predicted to precipitate. This is consistent with the observation (Appendix 5, IFESEM/EDS analysis) that copper is present in the iron-oxide mineral coatings (Appendix 5).

7 Discussion

7.1 Acid production

The variations in chemistry between deep and shallow groundwater in the delta is thought to be related to oxidation of the upper layer of groundwater (10 to 15 cm) by diffusion of oxygen from the atmosphere. Oxidation of aqueous ferrous iron will initiate precipitation of ferric oxyhydroxides, thereby producing acid. Decreases in aqueous metal concentrations will result from precipitation of iron-oxyhydroxides. Similar processes are expected to be occurring in the sediment banks. Oxidation of ferrous iron and precipitation of ferric oxyhydroxides not only describes the widespread iron-oxide staining and gradients in the groundwater chemistry, but may also explain the widespread acidity of some tailings-rich sediments that do not appear to contain significant amounts of pyrite or ferrous sulphate.

The general process of sulphide oxidation and acid production may be represented by the following equilibria based on pyrite oxidation and dissolution. Detrital pyrite in the tailings deposits is sporadically or continuously exposed to oxygen from the air, and decomposes to ferrous iron, sulphate and acid according to the following simplified reaction:

$$FeS_2 + 3.5\ O_2 + H_2O = Fe^{2+} + 2\ SO_4^{2-} + 2\ H^+ \qquad \text{Reaction 1}$$

Much of the groundwater in the delta and banks contains high ferrous iron concentrations, suggesting that this reaction is currently proceeding. As groundwater levels fluctuate, ferrous ions can be transported, for example, to higher levels in the delta. As the groundwater retreats, pores and grain surfaces will remain surrounded with groundwater containing the ferrous iron in the unsaturated zone. Oxidation of the iron in this residual water may be represented by the reaction:

$$Fe^{2+} + 0.25\ O_2 + H^+ = Fe^{3+} + 0.5\ H_2O \qquad \text{Reaction 2}$$

This reaction is slow, but may be catalysed by bacterial activity. High concentrations of ferric iron are unstable and the iron will tend to precipitate, eg as ferric hydroxide:

$$Fe^{3+} + 3\ H_2O = Fe(OH)_3(s) + 3\ H^+ \qquad \text{Reaction 3}$$

The combination of the reactions 1 to 3 produces 4 moles of acid for every mole of pyrite.

Partial dehydration of ferric hydroxide generates the ubiquitous orange Fe-oxide coatings over grain surfaces throughout the tailings deposits and pre-mine sediments:

$$Fe(OH)_3 = FeO(OH) + H_2O \qquad \text{Reaction 4}$$

Water coming into contact with the oxidised surface layers of sediment in the delta and banks becomes quite acidic (pH 2.5 to 3). Although this process is not understood, it may be due to hydrogen ions being liberated from the iron oxyhydroxide coatings. Goethite/lepidocrocite (FeOOH) likely precipitates as water evaporates from pore spaces leaving H^+ trapped or adsorbed onto ferric oxyhydroxide films. Later near-neutral rainfall displaces some of the H^+